Journal of Manufacturing Systems 74 (2024) 665–675

Contents lists available at ScienceDirect

Journal of Manufacturing Systems

journal homepage: www.elsevier.com/locate/jmansys

Technical paper

On the feasibility of an integrated English wheel system

Derick Suarez [a], Fan Chen [a], Putong Kang [a], Ben Forbes [a], Margaret Gao [a], Orlyse Ineza [a], Kevin Benton [b], Nicholas Dewberry [b], Chandra Jaiswal [b], Balakrishna Gokaraju [b], Kornel Ehmann [a], Jian Cao [a,*]

[a] *Department of Mechanical Engineering, Northwestern University, 633 Clark St, Evanston 60201, United States* [b] *Department of Computational Science & Engineering, North Carolina Agricultural and Technical State University, 1601 E Market St, Greensboro 27411, United States*

ARTICLE INFO

Keywords:
Flexible Metal Forming Automation
Digital Manufacturing
Industry 4.0

ABSTRACT

The English wheel is a highly flexible traditional metalworking tool that allows skilled craftsmen to form compound curves on sheet metal panels. Historically, geometric accuracy and repeatability of formed panels using the English wheel have been tied to the operator leading to limited industrial adoption. This paper presents a novel framework for an integrated English wheeling system that leverages robot forming with a newly developed adaptable gripper/end-effector, metrology for deformed geometry tracking and tolerance measurements, integrated sensors for real-time forming force measurements and control, computational modeling for tracking pattern/toolpath generation, and virtual reality (VR) for seamless integration. Sample panels are formed using the integrated system revealing new insights on the forming forces during the process – highlighting why an integrated system is desirable. Concepts from the proposed framework can be applied to other robotic forming processes and its merit is discussed under current digital manufacturing and industry 4.0 literature.

1. Introduction

Metalworking has been developed throughout human history, dating back to the oldest preserved Neolithic copper axe over 5000 years ago [1]. Today, it occupies a pivotal position in modern industry, contributing significantly to the economic prosperity of industrialized nations. The past century witnessed a seismic shift in metal-forming practices, driven by analytical studies and the advent of automation techniques. What once relied on skilled craftsmen/artisans in machine shops employing general-purpose tools has evolved into the realm of automated mass production, guided by specialized machinery, and dies. This evolution promised efficiency and scalability, yet it also ushered in a set of challenges that have become increasingly apparent in contemporary industrial landscapes. With the trend of personalized production [2], mass production methods have found themselves confronting a series of limitations such as lack of customization, high initial capital investment, long lead times, and environmental sustainability concerns. As such, various attempts have been made to include flexibility and resiliency in manufacturing [3,4], including proposed methodologies for changeable and reconfigurable manufacturing systems [5]. Such changeable systems stand to benefit from die-less and general-purpose tooling-based manufacturing processes.

To address limitations in flexibility, traditional processes have begun to be reexamined [6]. Traditional processes hold the advantage of added flexibility and cost-effectiveness provided by general-purpose tools/machines, but the inherent coupling with the operator often renders them unsuitable for modern industrial production. A recent review paper [7] summarizes the state of the art of incremental sheet forming and incremental bulk forming. To enhance the versatility of these incremental forming methods, researchers have introduced a suite of innovations, including the integration of multiple tools and robotic assistance. This transformation is underpinned by the aid of more precise automatic control, more realistic numerical and AI-based models, and advanced sensors, so called smart manufacturing [8] and Industry 4.0 [9].

Among the traditional metalworking methods [6] - which encompass an array of techniques including but not limited to hammering, shrinking/stretching, and spinning - the English wheel process stands out as uniquely capable of crafting compound curvature sheet metal panels. This apparatus (Fig. 1), marked by its simplicity, consists of a cylindrical upper wheel and a doubly-curved lower wheel (often referred to as the anvil) held together by a C-shaped frame. While both wheels are free to

* Corresponding author
E-mail address: jcao@northwestern.edu (J. Cao).

https://doi.org/10.1016/j.jmsy.2024.04.022 Received 18 April 2024; Accepted 19 April 2024
Available online 4 May 2024

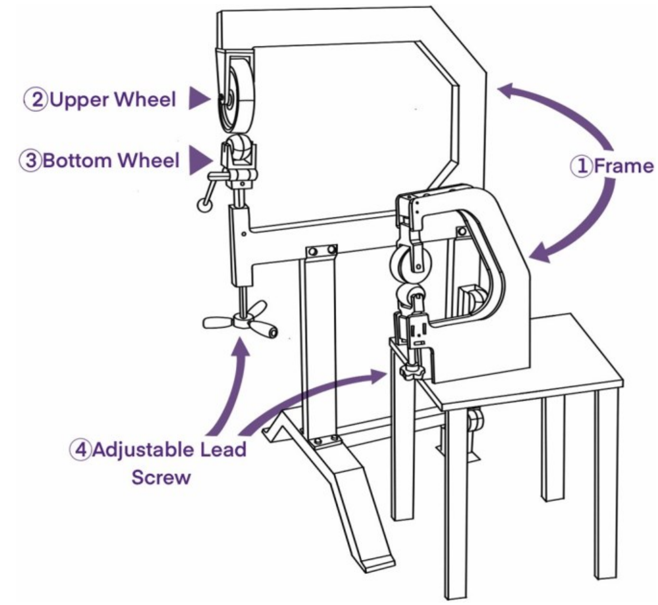

Fig. 1. Traditional English wheels are shown. Key elements are labelled. Larger English wheels typically boast larger forming forces as the frame is stiffer. Mini- English wheels have the advantage of being able to form smaller parts.

Fig. 2. High curvature panels manually formed with the English wheel. Fender- like objects are the desired target parts to show the capability of an integrated English wheeling system in the future. To make a complex piece like a fender through robotic forming, integrated components are essential.

rotate, the upper wheel remains vertically fixed, featuring a flat profile. Conversely, the anvil wheel can be vertically adjusted via a lower shaft, controlling the compressive force. Similar to other manual manufacturing techniques, the coupling of the operator in the English wheeling process limits industrial adoption. The craftsman actuates/drives the sheet (while engaged between the two wheels) through a series of paths – referred to as tracking pattern or toolpath in this paper – for which the craftsman often relies on years of experience. Fig. 2 depicts high curvature panels made manually through the English wheeling processes. While attempts at modernizing traditional processes have been performed – robotic hammering [10], robotic bead rolling [11], automated driving [12,13], and flexible asymmetric spinning [14] – the English wheel has only recently gained attention.

Rossi et al. [15] first proposed a cyber-physical system for the English wheel within an architectural lens, utilizing a robot arm for forming. Moreover, utilizing a limited dataset they showed the promise of using convolutional neural networks to address the forward problem (predicting panel deformation) and inverse problem (toolpath design) [16]. Bowen et al. [17] performed Finite Element Method (FEM) simulations using Abaqus, focusing on a single-track (linear path) and single-pass (no repeated track cycles) toolpaths with varying process parameters including reduction ratio and wheel radii. Typically, the reduction ratio (percentage change in sheet thickness) is prescribed through displacement boundary conditions on the wheels. However, such a method is hard to experimentally verify as the reduction ratio will be influenced by wheel geometries, sheet material properties and thickness, and frame compliance. Fann [18] undertook FEM modeling of the English wheel using LS-DYNA, exploring more intricate toolpaths featuring sawtooth, triangular, and rectangular track patterns. The investigation encompassed a study of resulting curvatures by varying process parameters. Again, the prescription of the reduction ratio through displacement boundary conditions is used leading to exceedingly high reaction forces (in kN range) if an arbitrary reduction ratio is used. Fann et al. [19] continued their work, mounting an English wheel onto a universal testing machine while a linear rail actuates the sheet in-plane. Experimental results and FEM simulations showed consistency. However, the set-up was limited to 2D toolpaths that do not properly reflect the flexibility in the traditional process. Additionally, very high compressive forces (through the aid of the universal testing machine) were used which are not achievable by most English wheel frames. The impact of these high forces on surface smoothness was not discussed, which is typically controlled by the operator in the traditional process by running several passes at low compressive forces. Huang et al. [20], building on Rossi's idea, used a robotic arm to form English wheeled sheet metal panels, displaying the repeatability of robotic forming along with outlining an algorithm to generate an arbitrary 3D path for robotic English wheeling through a series of translations and rotations.

Still many knowledge gaps remain for forming complex English wheeled parts using robotic forming (like the ones shown in Fig. 2) including:

- Fundamental mechanics for multiple passes
- Path/toolpath design for complex parts
- Monitoring and control of forming forces
- Appropriate boundary conditions in experiments
- Appropriate boundary conditions in simulations
- Efficient simulations/modeling
- Metrology systems
- Feedback control

In this paper, the feasibility of an integrated English wheel is shown (Fig. 3). The proposed system is composed of two main loops: (1) the tool path loop and (2) the force control loop. In the tool path loop, the modern craftsman leverages computational modeling for an initial toolpath design, which a robot with a compliant gripper carries out causing deformation of the panel. Metrological components scan the deformed panel and feed the current shape of the panel back to the computational model. In the force control loop, the computational model prescribes whether compressive force and/or toolpath should be updated. A controller is used to adjust the bottom shaft, outfitted with a stepping motor, to a set compressive force interacting with the top load sensor. The modern craftsman can monitor the whole process through VR and interact as needed.

In Section 2, the components of the integrated English wheel system are discussed, both in a large traditional wheel and a mini wheel (Fig. 1). A UR5e robot arm with a novel compliant gripper is used for forming. Both wheels have been outfitted with a compressive load sensor. A stepping motor has been added to the bottom shaft of the lower wheel (in the large set-up). Initial metrological implementations on the smaller wheel and initial VR representation of the large wheel are discussed. Computational modeling of the English wheeling processes using FEM is outlined.

Section 3 outlines forming experiments run with the implemented

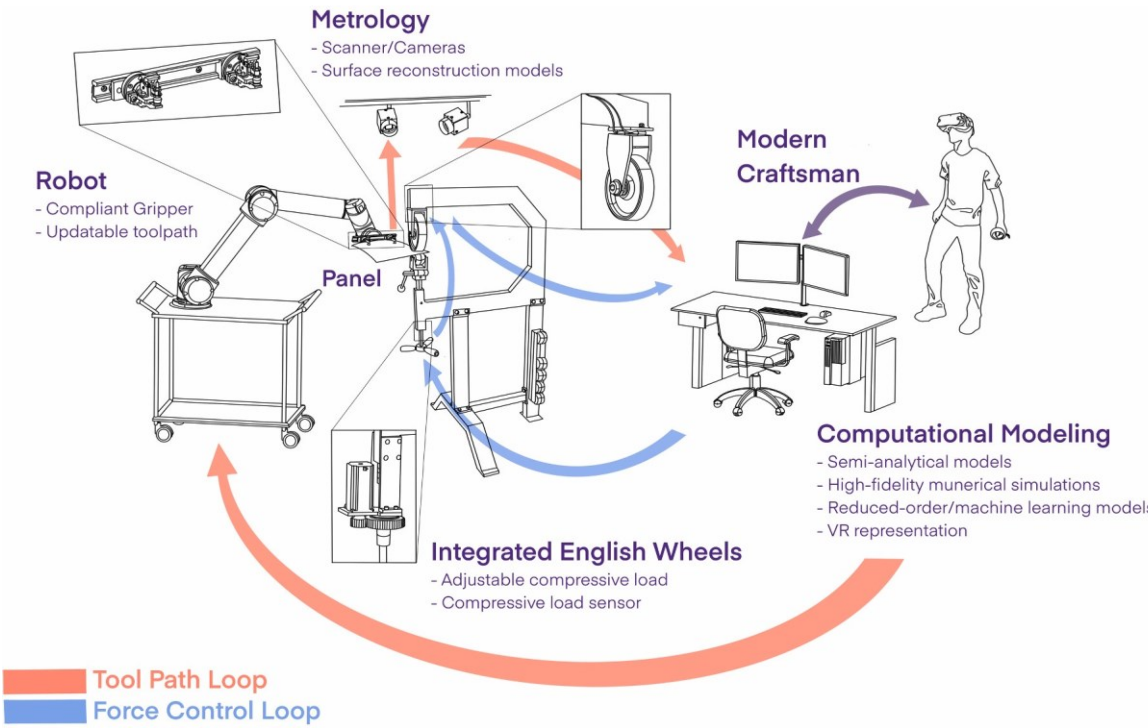

Fig. 3. Key components of the proposed integrated English wheeling system. A robot with a compliant gripper and updatable toolpath drives a sheet metal panel through an English wheel that has been outfitted with an automated adjustable bottom shaft to control the height of the bottom/anvil wheel and a compressive load sensor on the top of the frame to monitor forming forces. Metrological components in the form of scanners/cameras track the shape of the panel throughout passes which get fed into the computational modeling system. Here a combination of semi-analytical, numerical, and reduced order/machine learning models prescribe the toolpath for a desired final panel, taking the current shape of the sheet into account. The computational modeling module tracks the forming process and adjusts the forming forces in the wheel and updates the robot toolpath as needed. The modern craftsman monitors the whole process and can interact through VR.

components for single-track (linear) and multi-track (zig-zag pattern in this case) toolpaths. The experiments offer new insights on the forming forces during the English wheeling process and highlight the need for all the proposed components to be integrated. Selected experiments are used for validation of the FEM model proposed in Section 2.

Section 4 contains results on forming trials and subsequent discussions. Section 5 offers conclusions and ongoing/future work.

2. Integrated system

Two standard English wheels are used (shown in Fig. 1):

- The larger is a F.1 × 710 28-inch Throat English wheel manufactured by KAKA Industrial. The top/upper wheel has a lateral radius of 101.6 mm and a frontal width of 50.8 mm. The bottom/lower/anvil wheel is doubly-curved (lateral and frontal radii) and is interchangeable (different radii), with a frontal width of 50.8 mm.

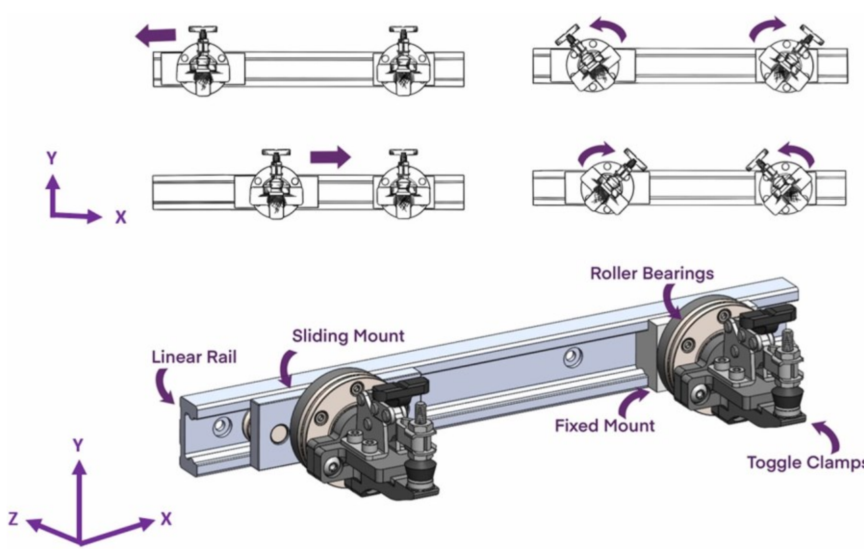

Fig. 4. Compliant gripper system with additional degrees of freedom (local axes shown). Both contact points (toggle clamps) are attached to bearings that can rotate about the z-axis. One of the contact points is translationally fixed, while the other can translate along the rail in the x-direction.

Fig. 5. The flexible gripper is shown being able to adapt to the shape of the sheet that has significantly deformed by the English wheel.

- The smaller is a 7.5-inch Throat Eastwood Elite Mini English wheel with an in-house modified frame (to accommodate a load sensor). The top/upper wheel has a lateral radius of 40.5 mm and a frontal width of 24.6 mm. The bottom/lower/anvil wheel is doubly-curved and is interchangeable, with a frontal width of 24.6 mm.

A description of the components of the integrated English wheeling system follows.

2.1. Compliant gripper

Both wheel systems use a custom end-effector/gripper made for the UR5e robot. In a static end-effector/gripper, the sheet metal is restricted from stretching and bending. This results in interference with the regular deformation of the sheet throughout the passes. To closely mimic the state of the held sheet when worked through the English wheel, linear and rotational degrees of freedom were designed into a new gripping system. The novel compliant gripper system, shown in Fig. 4 and Fig. 5, consists of two toggle clamps that grip the sheet metal at two edge locations/contact points. As the sheet metal is wheeled, the length of the gripped edge changes and assumes a curved shape. Both toggle clamps are mounted on cross-roller bearings, which enable the toggle clamps to rotate and match the angle of the sheet metal as it deforms. The left toggle mount and bearing system are attached to a linear rail. The linear rail enables the distance between the grippers to vary as the sheet metal is formed. The added linear and rotational degrees of freedom enable more flexibility when forming sheet metal components and allow for the forming of geometries that would not otherwise be possible.

Two high-load face-mount cross-roller bearings with 10 mm shaft diameters were chosen such that they could easily be bolted to the toggle clamp on one side and the linear rail on the other side. During normal English wheeling the primary loading on the gripper system is in the axial direction. In order to be fault tolerant, the gripper system must also withstand moment and radial loads. Cross-roller bearings were chosen due to their ability to support combined axial, radial, and moment loads. Two compact hold-down toggle clamps with rubber contact points were used to minimize the distance from the mounting point to the grip contact location. The toggle clamps were fastened to custom designed mounts that were manufactured by fused filament fabrication out of PLA on a Fortus 3D printer with 100% infill. These toggle clamp mounts were then bolted to the bearings. Two additional customized fixtures were used: one was used to fasten one of the bearings to the track roller carriage, and the other to the linear guide rail. Fig. 5 shows the compliant gripper in action, being able to accommodate the curvature of a formed English wheeled panel.

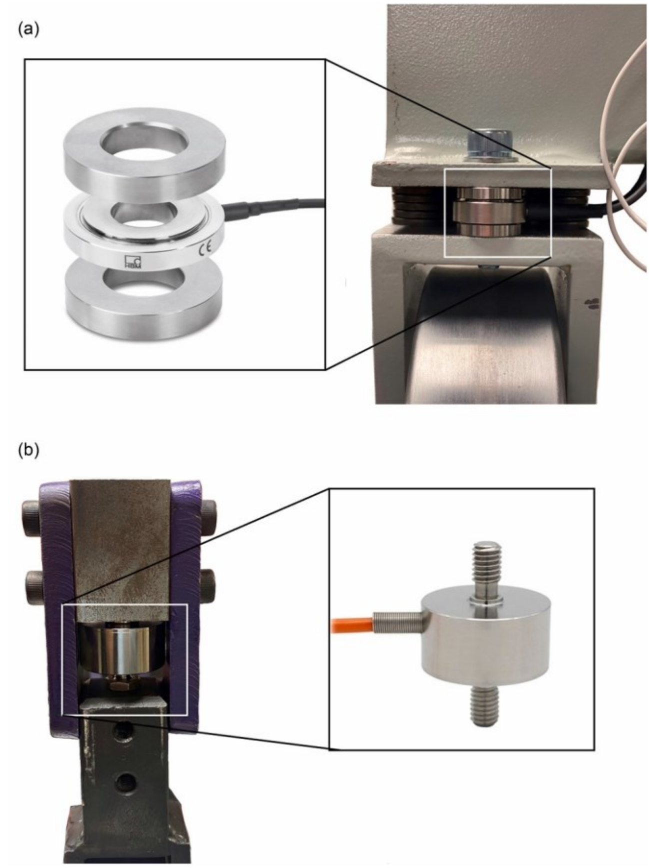

Fig. 6. Load sensors on the large wheel (top, only front sensor shown) and mini wheel (bottom). Note that additional structural washers (not load sensors) were placed along the two force washers to increase stability and levelness on the large wheel.

2.2. Load measuring system

Compressive load sensors were integrated into the large and mini- English wheels (Fig. 6). While lateral forces are present (in the direction of driving), compressive forces (axial) directly affect how much deformation occurs in the sheet. In the limited English wheeling literature, the reduction ratio is used as a method for controlling the process, particularly in simulation [17,18]. However, measuring the reduction ratio is cumbersome. A more natural measurement is the compressive load acting on the sheet. Moreover, single-axis sensors boast low cost and ease of integration. Both load sensors use a TDK DRB30–24-1 AC-DC power supply and utilize LabVIEW scripting to output voltages using an NI cDAQ-9172 chassis and NI 9215 card.

- For the large wheel two 1-KMR+ /60KN HBM force washers along with two Advantech ADAM-3016 isolated strain gauge input modules were used. The washers were placed between the top plates of the wheel with threads going through them. Calibration was performed by first removing the wheels and attaching a pre-calibrated Kistler 9273 multi-component dynamometer to the top of the frame. A steel bar was placed between the bottom of the frame and the dynamometer. A dial gauge was used to measure the deflection of the frame as the bottom shaft was used to squeeze the steel bar tighter, resulting in a force-displacement curve (stiffness of the frame) – this relationship was linear. 4.5 kN was near the maximum the frame could withstand without onsetting damage to the structure. The dynamometer was then removed, and the wheels and force washers were placed back in the frame. Using the same dial gauge, a voltage-displacement curve was generated by squeezing the wheels together at various amounts and recording the output voltage from the washers. Then, the final force-voltage curve for the washers was generated by matching displacements with the stiffness of the frame curve.
- For the smaller wheel a DYMH-103 100 kg Mini Tension and Compression Force Sensor Load Cell was built into the modified frame, and a Caltsensor Load Cell Weight Transmitter Amplifier JY- S60 Series was used. The modified mini wheel frame contains two mounts with tapped holes that allow the load cell to be placed above the upper wheel. The load cell was calibrated by placing known loads on the mounts (while the load cell was not mounted on the wheel) and reading the voltage output. This process was repeated three times to create a force-voltage curve – exhibiting linear behavior.

2.3. Automated anvil adjuster

The anvil wheel on the large English wheel is adjusted using a geared stepper motor that rotates the existing lead screw (Fig. 7). A NEMA 23 stepper motor drives a geartrain with a gear ratio of 3:1. The gear rotates a ball spline which is connected to a lead screw integrated into the bottom of the English wheel. The lead screw then raises and lowers the wheel to a desired location based on the force being applied to the sheet metal. The stepper motor is driven by a StepperOnline DM542T digital stepper driver receiving commands from a NU32 microcontroller. The microcontroller implements a force control system based on the feedback from the force washers mounted on the large wheel. The microcontroller, yet to be implemented, will take a desired input force, and then use proportional control to raise the anvil wheel until that force is reported by the load washers. The method of force feedback is very similar to the manual system, in which the lead screw raises and lowers the lower wheel to a prescribed location by the craftsman, who can feel the force being exerted on the sheet metal. The goal of the system is to use the mechanical force feedback system to actively control the amount of force being exerted on the sheet metal at any given time during the toolpath. Changing the force within the toolpath allows an additional parameter affecting the final geometry of the sheet metal part.

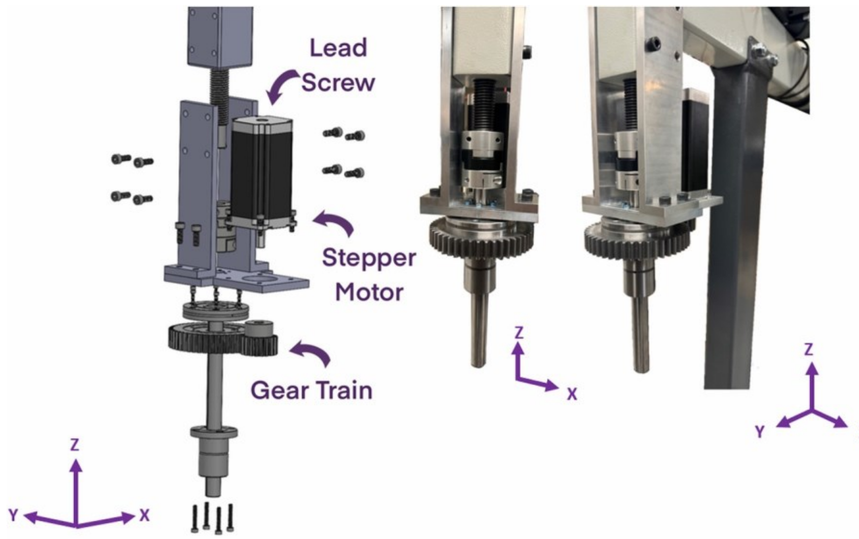

Fig. 7. Anvil adjuster CAD (left) and system installed on the large English wheel (local axes shown).

2.4. Metrology system

An initial metrological system for the mini-English wheel has been implemented. This system consists of a Vicon motion capture system, equipped with 6 infrared cameras. Based on optical tracking, the system records the three-dimensional movement paths of reflective markers that are placed on the surface of the sheet. The sheet shape can then be reconstructed using the marker locations. Zhang et al. [21], demonstrate the usability of the system. However, limitations exist. The use of markers naturally interferes with the forming process, so the markers need to be placed on the forming area after the completion of a forming cycle. Additionally, the accuracy of the shape reconstruction can be further improved. Reconstruction of the sheet shape is necessary for the toolpath update loop within the integrated system. In the manual process, the craftsmen adjusts gripping and toolpath as the sheet gains curvature. The same is hoped to be replicated in robot forming through accurate metrological systems. Without updating toolpaths to consider high curvature changes in the sheet, the robot arm will forcibly jam the part through the wheels causing a load-out.

2.5. Computational modeling

High-fidelity FEM models are used to predict the forward problem (predicting the final shape based on the toolpath). Bowen et al. [17] modelled single-track and single-pass English wheeling cases by prescribing the reduction ratio. Prescribing the force is an alternative used in this paper. In Fann's multi-track simulations [18], reduction ratios were set as high as 50% for a 1 mm DC04 sheet resulting in compression forces in the range of 30 kN. As evidenced by the stiffness measurement of the large wheel frame described in Section 2.2, compressive forces held by the specific frame used in this study do not exceed 5 kN. However, such forces are manageable if the English wheel is mounted on a universal testing machine as in Fann's subsequent work [19]. Still, simulation for complex 3D paths has not been performed and is an ongoing challenge due to difficulties in prescribing boundary conditions to enforce toolpaths.

Key considerations for a single-track path are shown in Fig. 8(a) - these and others can be extended to multi-track paths and 3D paths. Modeling of the English wheel process can be split into 3 phases: (1) engagement, (2) actuation/forming, and (3) springback.

- Implicit, dynamic implicit or explicit FEM solvers can be used. Following standard metal forming practices (where inertia is important), explicit simulations are chosen for engagement and actuation/forming for this paper while for springback the simulation can be switched to implicit or kept in explicit if oscillations are damped out.
- During engagement, reduction ratios can be enforced by applying displacement boundary conditions on the wheels to achieve the desired clearance. Alternatively one can model spring elements on the wheels and define stiffness. For the large wheel in this study as described in Section 2.2, the calculated stiffness of the frame is 800 N/mm. If the initial applied load is known (as is the case with integrated wheels thanks to the sensors added), then it is straightforward to prescribe the force.
- During actuation, the sheet is gripped at one or more contact points, and then driven by the robot arm. One can use standard kinematics to define a hold region and apply displacement/velocity boundary conditions on this hold region. For multi-track patterns, additional steps of rotation are implemented. Note that this rotation should be centered around the contact point of the sheets and wheels, not the hold region. The wheels can be given mass/inertia to be able to rotate freely due to friction interactions. Alternatively, one can create an equivalent model where the displacement/velocity boundary conditions are applied on the wheels themselves while the sheet is fixed at grip contact points. In this case, the wheels can also have free rotation, or a known rotational velocity can be prescribed. The equivalent model lends itself well to single-track toolpaths and is utilized in this paper.
- Solid elements provide a higher degree of accuracy compared to shell elements but come at additional computational expense. The wheels are modelled as rigid. "Hard" contact is established between the sheet and the top/bottom wheel in ABAQUS, along with friction. The mesh size of the wheels and sheet should be sufficiently fine near the forming areas to capture the curvature of the anvil wheel. Five solid elements are used in the through-thickness direction in this work. Fig. 8(b) depicts FEM models.
- Advanced material models have been shown to directly impact the accuracy of forming simulations, particularly springback [22,23]. In the present study, uniaxial data for 316 L stainless steel [24] was used, with isotropic hardening and a Mises yield criterion. Future work will include characterization of the precise 316 L stainless steel used to include non-isotropy and kinematic hardening effects.

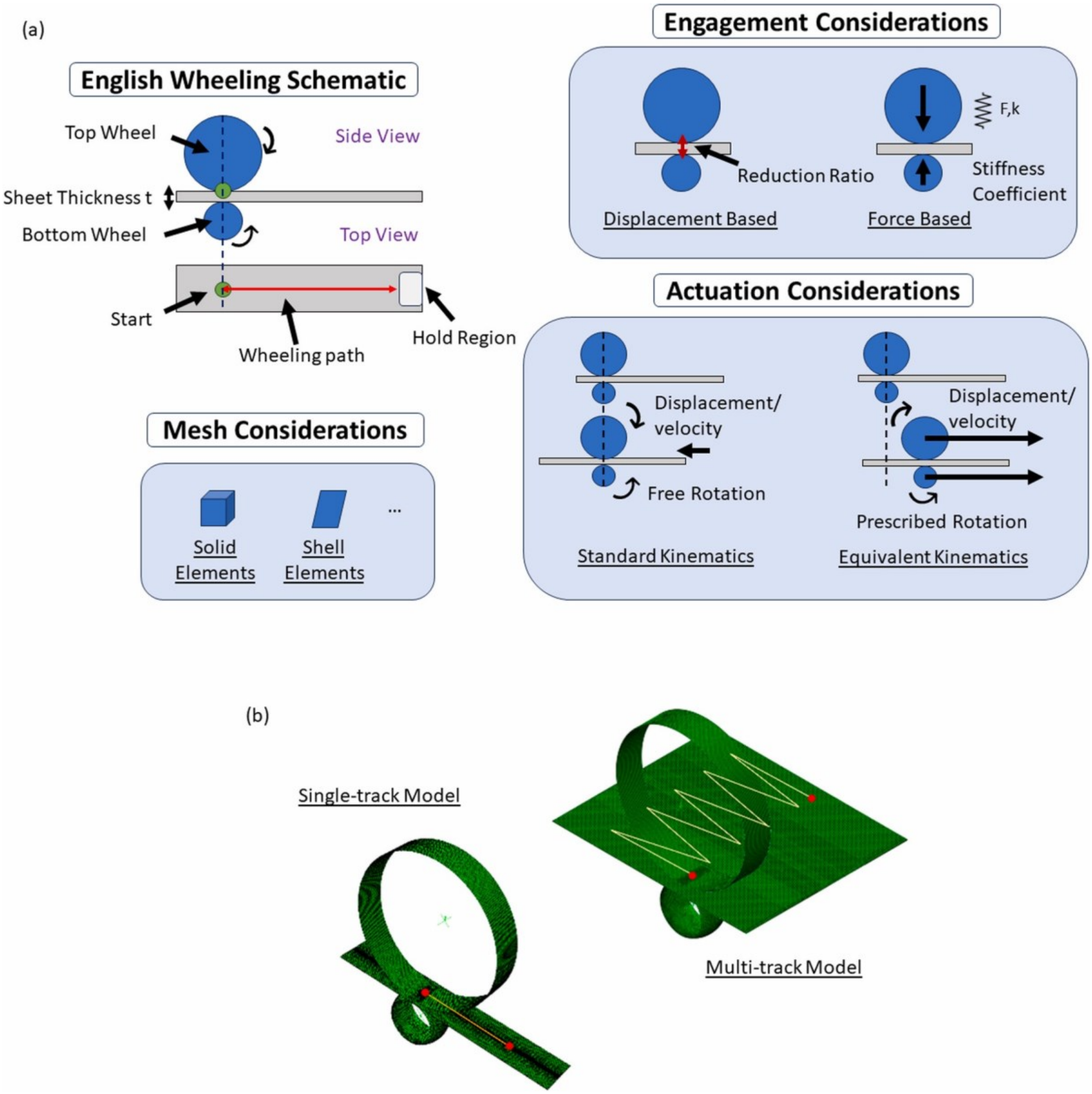

ig. 8. (a) Key considerations when modeling single-track English wheeling: (1) definition of sheet engagement/compression, (2) mirroring the real-world kinematics or applying equivalent oundary conditions, and (3) choice of element type/meshing. (b) ABAQUS FEM models for single-track and multi-track wheeling. Equivalent model where displacement is prescribed n the wheels instead of on the sheet is used.

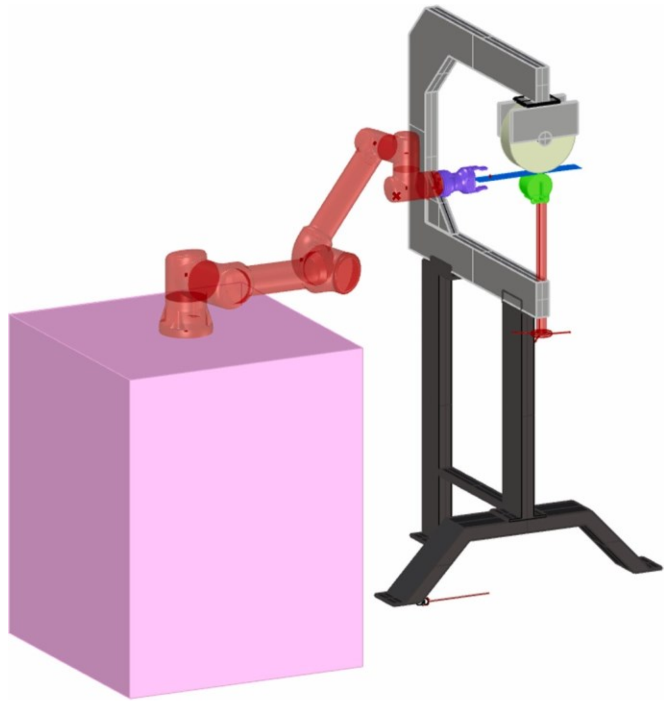

Fig. 9. VR representation of English wheel robotic forming using Rhino 3D.

2.6. VR representation

An initial VR representation of the large English wheel system has been implemented (Fig. 9). The VR model was created using Rhino 3D. Physical measurements were taken of the English wheel and relevant components, which were used create a virtual counterpart within Rhino 3D. The robot arm was imported using the Robots plugin. The UR (Universal Robot) script files, which drive the toolpath of the robot in the physical world, are imported directly. Ongoing implementations of how to define the metal sheet and its subsequent deformation are being explored. A virtual environment, accessible through a VR device, was generated using the Fologram plugin. Benton et al. [25] highlight an in-depth description of the VR methodology along with possible interactions between the physical and virtual world during the integrated wheeling process.

3. Application of integrated system

Experimental trials were performed to show forming forces during the process and parameter influence on the final curvature of the part. All experiments were performed using 0.6 mm thick 316 L stainless steel sheets and using the UR5e robot arm and flexible gripper described in Section 2.1 (single-track and multi-track samples use 1 and 2 grip points, respectively).

Sheet geometries and toolpaths used are shown in Fig. 10. A cycle is defined as following the tracking pattern/toolpath (shown in red) and returning to the initial position (shown in green). Returning to the initial position follows the reverse tracking pattern with the wheels still engaged. Load data is collected through the sensors described in Section 2.2 at a rate of 100 Hz, where appropriate. Huang et al. showed that the robotic wheeling process has good repeatability subject to accurate initial starting point alignment between the sheet and wheel [20], as such only one sample is wheeled under the following conditions.

Trial 1 uses the mini-English wheel. Trial 1 is used to gain insights into the experimental forming forces, which have been previously unexplored. Details are as follows:

- **Case A**. One sample, each, for geometry/toolpath a) for 5 cycles (5 s pause between cycles) at.
- 250 N using robot forming.
- 600 N using robot forming.
- 250 N using manual wheeling.
- **Case B.** One sample, each, for geometry/toolpath b) for 1 cycle at.
- 250 N using robot forming.
- 400 N using robot forming.
- **Case C.** One sample for geometry/toolpath c) for 1 cycle at.
- 250 N using robot forming.

Trial 2 uses the large English wheel. Trial 2 is performed to see the influence of compression force at a larger scale than the mini wheel (the mini wheel can only achieve relatively low forces) and demonstrate FEM modeling potential (the larger size of the wheels leads to large mesh sizes, making simulations more computationally friendly). Details are as follows:

- **Case A.** One sample, each, for geometry/toolpath a) for 0.5 cycles at
- 1 kN using robot forming.
- 1.5 kN using robot forming.
- 2 kN using robot forming.

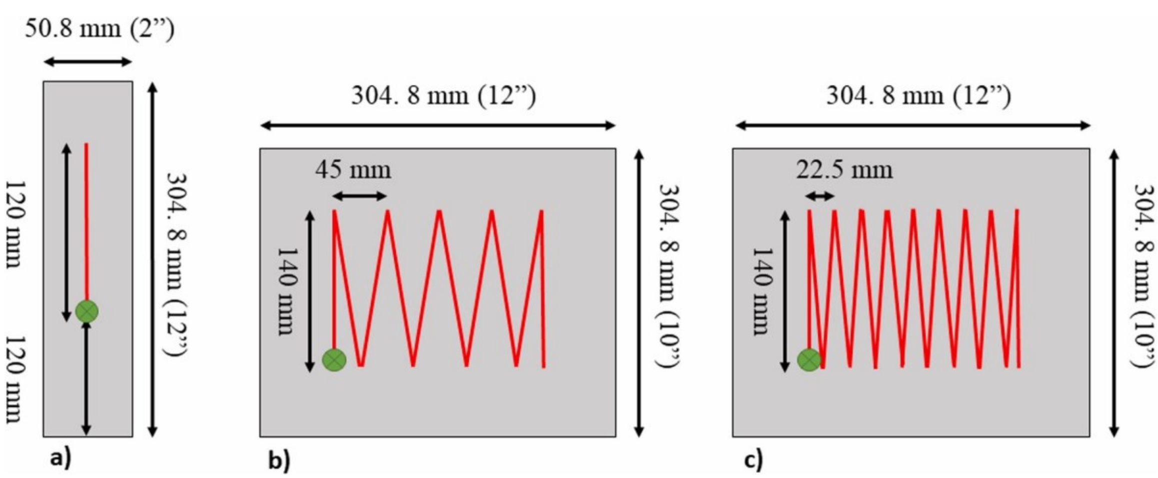

Fig. 10. Sample geometries and track patterns/toolpaths (red). For full cycle, the sheet is wheeled through the track pattern starting at the initial position (green) towards the red path. The sheet is then wheeled through the track pattern in reverse to arrive at the initial position.

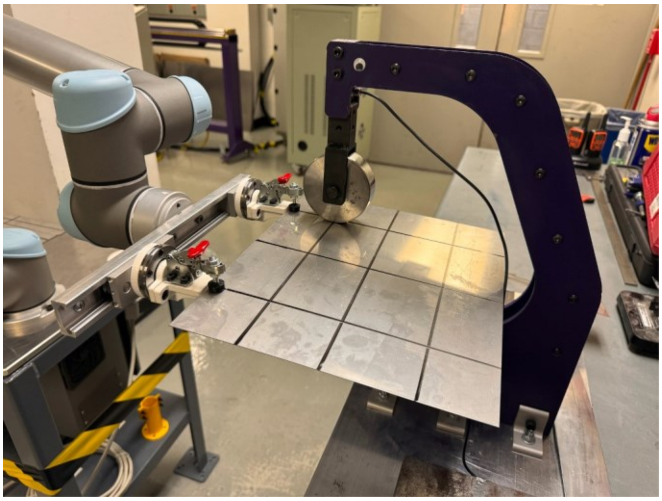

Fig. 11. Initial set-up for robot forming utilizing the mini-English wheel.

4. Result & discussion

4.1. Trial 1

Fig. 11 is a snapshot taken before the forming of one of the cases in Trial 1. The top graph (a) in Fig. 12 reports the load readings for Trial 1 Case A. Focusing attention on the case where the initial load reading was set at 600 N, one can see a large initial drop-off in the force when wheeling begins. Recall that this sample is a thin strip with one grip point (that has degrees of freedom due to the compliant gripper) for 5 cycles. As such some initial compliance in the set-up is expected. Once wheeling has begun a stable plateau of 300 N can be seen. Five (5) trough/crest pairs can also be seen. These correspond to the 5 forming cycles. It is surmised that due to the in-line 1D (axial) nature of the load sensor when the sheet is pushed inwards and outwards, slight moments are imparted resulting in the through/crest features seen in the graph. Nevertheless, the readings provide valuable insight into average forming forces occurring during English wheeling. Multi-directional sensors can be implemented in the future to better decouple the forming forces. Looking at the 250 N case, a similar trend to the 600 N case is seen, albeit at a lower force. A 250 N case was performed manually and compared to the 250 N robot forming case. One can see that even for this straight-forward linear-tool path, the manually formed load reading is much less consistent than the robot-formed one.

The resulting deformation for Trial 1 Case A is very low as the load is low and the toolpath is small and linear. A more representative toolpath, zig-zag, is used in Trial 1 Case B shown in the middle graph (b) of Fig. 12. Here both grips/toggle-clamps of the flexible gripper are used, leading to a much more stable initial configuration causing the previous initial load drop-off to vanish. Trough/crest pairs corresponding to the number of segments formed are seen. Of note, for both the 250 N and 400 N cases, the final load reading is lower than initial. Vibrations in the system can potentially loosen the tightness of the wheels. Additionally, as the sheet deforms, the gripping contact points can rotate and translate which can result in a different sheet-wheel contact configuration affecting the load. Mitigating this load decrease will be handled by the motorized shaft of the anvil wheel discussed in Section 2.3.

Even for the more representative zig-zag pattern, deformation of the sheet is relatively low even when raising the force. Another method to get increased deformation is increasing the tightness of the zig-zag pattern (decreasing the spacing, previously 45 mm now 22.5 mm in Trial 1 Case C). The closer subsequent forming segments are the more plastic deformation overlap is present, leading to a larger global curvature. The bottom graph (c) in Fig. 12 reports the load readings for Trial 1 Case C. Fig. 13 plots the out-of-plane contours for Cases B and C.

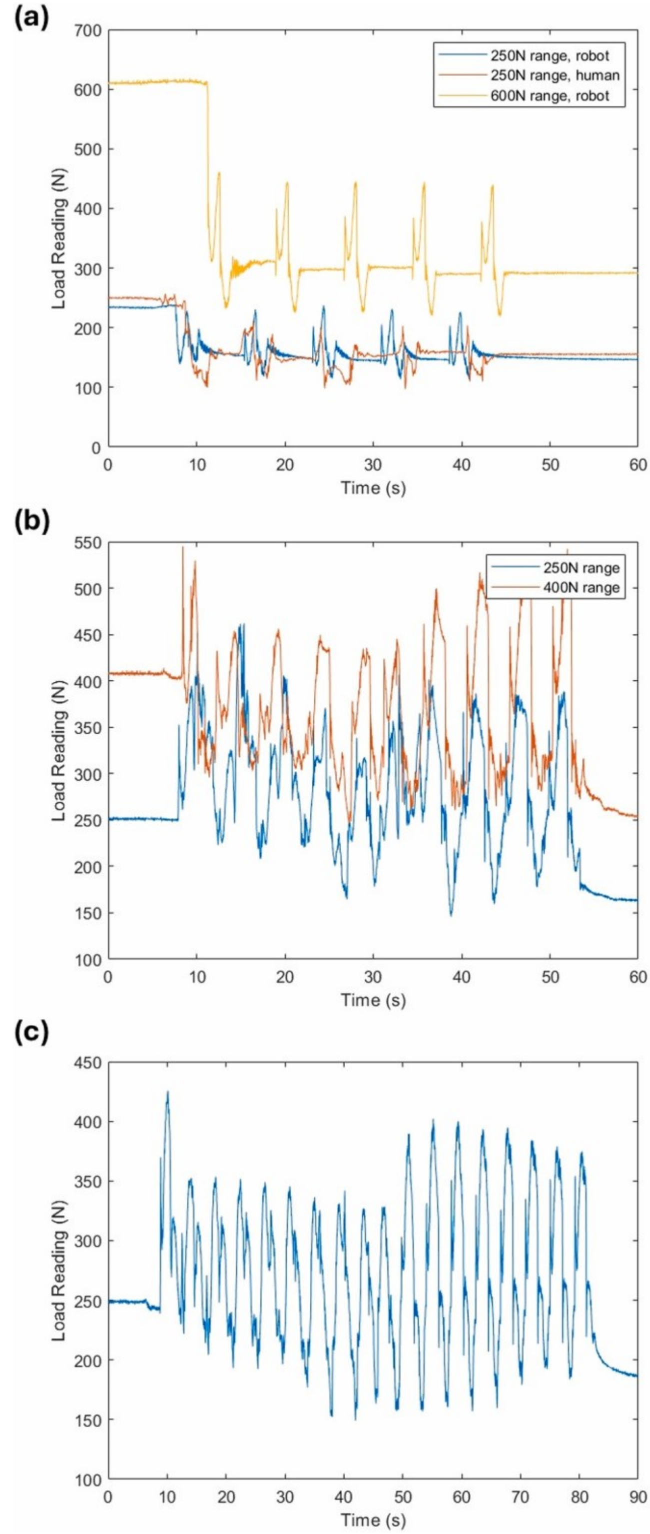

Fig. 12. Loads in Trial 1. The top, middle, and bottom graphs correspond to Cases A, B, and C, respectively.

One can see two avenues of increasing global curvature: increasing force, or alternating toolpath. This reflects the philosophy in the integrated English wheeling system proposed in Fig. 3: a tool path loop and force control loop.

Fig. 13. Out-of-plane contours for Trial 1 Cases B and C. Taking the center panel as reference one can see that increasing the applied load (left) only marginally changes the profile (due to the relatively low change in force magnitude that is possible with the mini wheel), while changing the zig-zag spacing (right) has a much

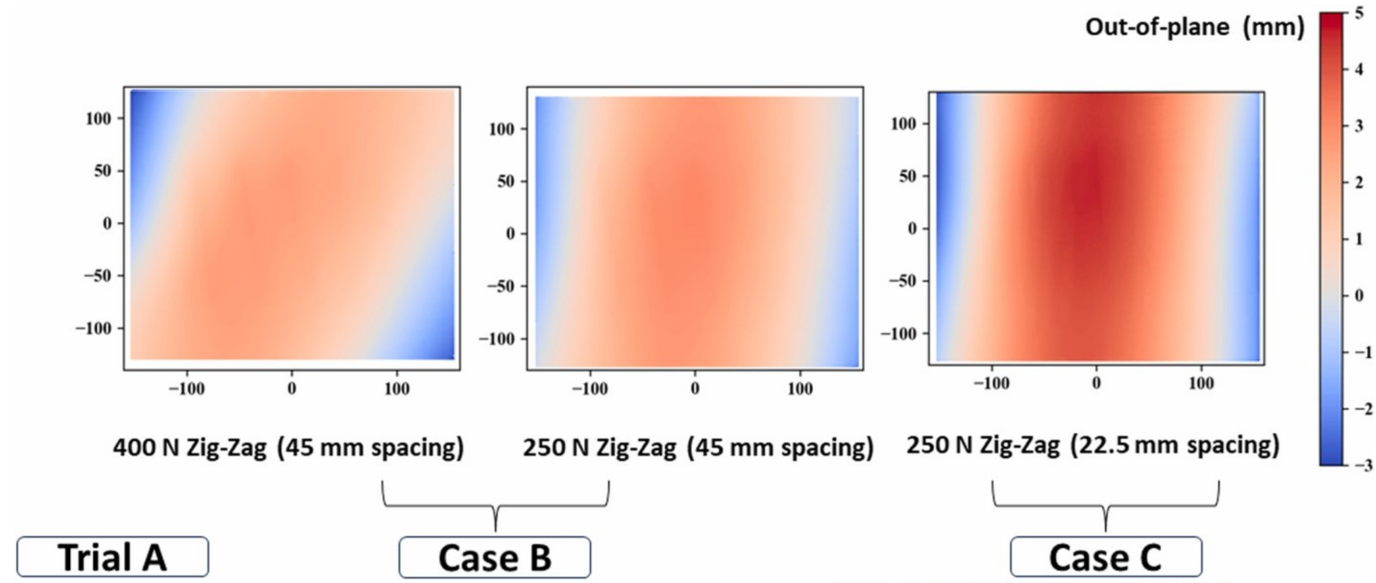

more pronounced effect.

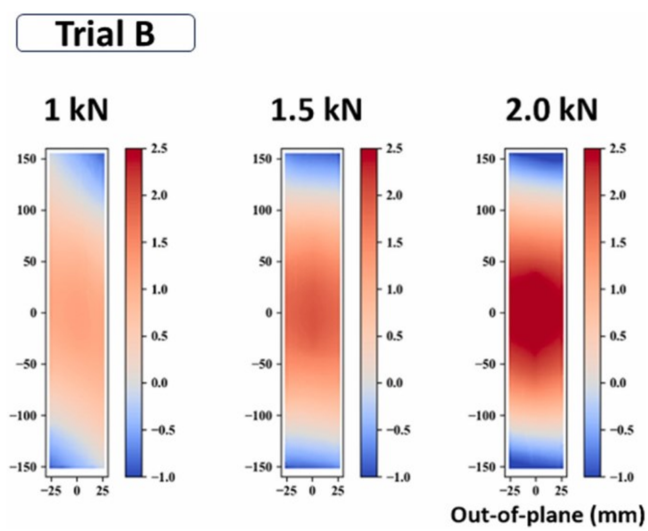

Fig. 14. Influence of the forming force. A larger forming force leads to greater global deformation.

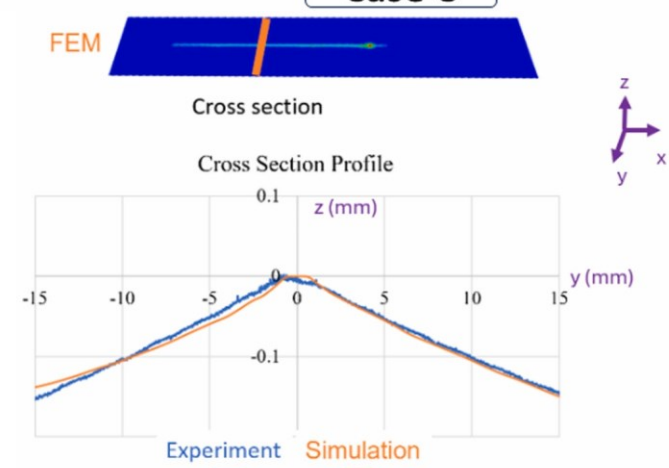

Fig. 15. FEM simulated and experimental cross section profiles for a 2 kN sample match well.

4.2. Trial 2

Out-of-plane contours for Trial 2 Case A are shown in Fig. 14. Based on the applied loads, one can see that the larger wheel is capable of forces in the low kN. While the calibration discussed in Section 2.2 saw the frame max out around 4.5 kN, hand wheeling is nearly impossible around that range and the robot arm will also max out due to large lateral forces. From Fig. 14 one can see that increasing loading is a viable way to increase the global curvature in a wheeled part. Lastly, in Fig. 15, the 2 kN experimental sample is compared against simulation. A cross- section profile is plotted showing agreement between the two.

4.3. Manufacturing applicability

Sun et al. recently performed a bibliometric study on the digital twin (DT) research for the last 20 years in which potential hotspots and frontiers are highlighted within 4 categories: Basic Technology, Application Development, Specific Implementation, and Auxiliary Technology [26]. The integrated English wheeling system presents potential advances in all of these categories. Within Basic Technology the ongoing development of an extended reality version of the English wheel through VR poses an avenue for both workforce development and educational teaching. De Giorgio et al. outline the potential benefits of VR in being able to convey near-real manufacturing environments without impacting the manufacturing line [27]. However, most current examples are prototype scale and lack proper testing. Cimino et al. identified key barriers to VR and DT adoption including the need for ready-to-use application, interoperability, and comprehensive platforms [28]. The proposed VR component of the integrated English wheeling system aims at building a comprehensive ready-to-use application (Application Development) that is tested against real manufacturing environments [25]. Further development in Basic Technology is planned by developing new machine learning frameworks to monitor part tolerances in the Specific Implementation of English wheeling. Machine learning methods have gained popularity in online quality morning such as in robotic welding [29]. Such methodologies are planned to be adopted and updated to meet the need of surface reconstruction of sheet metal panels by training models on a database of common and known English panel geometries in the future. Auxiliary Technology such a numerical models and methods are continued to be developed to provide more insight into path planning during the English wheeling process.

5. Conclusions

A novel integrated English wheeling system was presented composed of two control loops: force control and toolpath generation. Implemented and planned components were outlined. A novel compliant gripper was demonstrated, being capable of conforming to the shape of wheeled panels. The presented gripper can be modified to fit other applications were the gripper contact location is subject to shape change. Integration of load measuring systems in English wheeling was demonstrated. For the first time, loading forming forces during the English wheeling process were reported. This insight can better inform FEM modelers of the process. An adjustable lower shaft anvil system was presented which will be integrated into the force control loop. Descriptions of ongoing work on metrology [21] and VR [25] compatibility were described. Fabrication of representative parts was performed showing the influence of the forming force and track pattern, highlighting the merit of having a fully integrated system. A discussion on FEM modeling was presented, along with a sample validation case.

Future work includes integrating the described systems to form complex parts like a motorcycle fender. This includes developing more robust computational models necessary for toolpath design, implementation of metrology systems that do not interrupt the forming process, shape reconstruction of deformed panels between cycles, feeding back into the computational model for adjustments, force control between the automated lower shaft and load sensors, and full integration of the system in VR. Methodologies implemented have the potential to be adopted to other robotic forming processes like robotic single point incremental forming (SPIF) [30].

CRediT authorship contribution statement

Orlyse Ineza: Data curation, Formal analysis. **Derick Suarez:** Formal analysis, Investigation, Methodology, Writing – original draft, Writing – review & editing. **Margaret Gao:** Investigation, Visualization. **Nicholas Dewberry:** Formal analysis. **Kevin Benton:** Investigation, Writing – original draft. **Balakrishna Gokaraju:** Conceptualization, Funding acquisition, Supervision. **Chandra Jaiswal:** Investigation. **Jian Cao:** Conceptualization, Funding acquisition, Project administration, Writing – review & editing. **Kornel Ehmann:** Conceptualization, Funding acquisition, Supervision, Writing – review & editing. **Putong Kang:** Conceptualization, Investigation. **Fan Chen:** Formal analysis, Validation. **Ben Forbes:** Formal analysis, Investigation.

Declaration of Competing Interest

The authors declare that they have no known competing financial interests or personal relationships that could have appeared to influence the work reported in this paper.

Acknowledgements

The authors would like to acknowledge support from the NSF Engineering Research Center for Hybrid Autonomous Manufacturing Moving from Evolution to Revolution (ERC-HAMMER) under Award Number EEC-2133630. The authors would also like to acknowledge the Northwestern Class of ’23 Mechanical Engineering (ME) seniors and instructors who partook in the senior ME design capstone class (winter- spring) and developed the compliant gripper.

References

[1] Cao J, Banu M. Opportunities and challenges in metal forming for lightweighting: review and future work. J Manuf Sci Eng 2020;142:110813. https://doi.org/ 10.1115/1.4047732.

[2] Berry C, Wang H, Hu SJ. Product architecting for Personalization. J Manuf Syst 2013;32:404–11. https://doi.org/10.1016/j.jmsy.2013.04.012.

[3] Zheng P, Xu X, Yu S, Liu C. Personalized product configuration framework in an adaptable open architecture product platform. J Manuf Syst 2017;43:422–35. https://doi.org/10.1016/j.jmsy.2017.03.010.

[4] Ren X, Zhao N. Research on digital twin framework for customized product manual assembly systems. J Manuf Syst 2023;71:527–45. https://doi.org/10.1016/j.jmsy.2023.08.018.

[5] Andersen R, Napoleone A, Andersen A-L, Brunoe TD, Nielsen K. A systematic methodology for changeable and reconfigurable manufacturing systems development. J Manuf Syst 2024;74:449–62. https://doi.org/10.1016/j.jmsy.2024.04.008.

[6] Bowen DT, Russo IM, Cleaver CJ, Allwood JM, Loukaides EG. From art to part: Learning from the traditional smith in developing flexible sheet metal forming processes. J Mater Process Technol 2022;299:117337. https://doi.org/10.1016/j. jmatprotec.2021.117337.

[7] Yang DY, Bambach M, Cao J, Duflou JR, Groche P, Kuboki T, et al. Flexibility in metal forming. CIRP Ann 2018;67:743–65. https://doi.org/10.1016/j.cirp.2018.05.004.

[8] Lu Y, Xu X, Wang L. Smart manufacturing process and system automation – a critical review of the standards and envisioned scenarios. J Manuf Syst 2020;56:312–25. https://doi.org/10.1016/j.jmsy.2020.06.010.

[9] Xu X, Lu Y, Vogel-Heuser B, Wang L. Industry 4.0 and industry 5.0—inception, conception and perception. J Manuf Syst 2021;61:530–5. https://doi.org/10.1016/j.jmsy.2021.10.006.

[10] Ilangovan B, Monfared RP, Jackson M. An automated solution for fixtureless sheet metal forming. Int J Adv Manuf Technol 2015;82:315–26. https://doi.org/ 10.1007/s00170-015-7366-x.

[11] Friedman J., Hosny A., Lee A. Robotic Bead Rolling. Proceedings of the 34th Annual Conference of the Association for Computer Aided Design in Architecture (ACADIA) 2014. doi:10.52842/conf.acadia.2014.231.

[12] Opritescu D, Sachnik P, Yang Z, Golle R, Volk W, Hoffmann H, et al. Automated driving by standardizing and scaling the manufacturing strategy. Procedia CIRP 2012;3:138–43. https://doi.org/10.1016/j.procir.2012.07.025.

[13] Hartmann C, Opritescu D, Volk W, Schmiedl F, Ritter M, Gritzmann P. A knowledge-based automated driving approach for flexible production of individualized sheet metal parts. Knowl-Based Syst 2022;244:108558. https://doi.org/10.1016/j.knosys.2022.108558.

[14] Music O, Allwood JM. Flexible asymmetric spinning. CIRP Ann 2011;60:319–22. https://doi.org/10.1016/j.cirp.2011.03.136.

[15] Rossi G, Nicholas P. Modelling a complex fabrication system - new design tools for doubly curved metal surfaces fabricated using the English wheel. eCAADe Proc 2018. https://doi.org/10.52842/conf.ecaade.2018.1.811.

[16] Rossi G., Nicholas P. Re/learning the wheel. methods to utilize neural networks as design tools for doubly curved metal surfaces. Proceedings of the 38th Annual Conference of the Association for Computer Aided Design in Architecture (ACADIA) 2018.

[17] Bowen DT, Music O, Alaz Erdinc A, Shokrani A, Loukaides EG. Numerical Modelling and Deformation Mechanics of the English Wheel Process. In: Daehn G, Cao J, Kinsey B, Tekkaya E, Vivek A, Yoshida Y, editors. Forming the Future. Cham: Springer International Publishing; 2021. p. 457–66. https://doi.org/10.1007/978- 3-030-75381-8_38.

[18] Fann KJ. Finite element study on forming metal sheets with an english wheel. IOP Conf Ser: Mater Sci Eng 2022;1222:012006. https://doi.org/10.1088/1757-899X/1222/1/012006.

[19] Fann K-J, Wu Y-H. On forming sheet metal parts in single curvature with English wheel. Lect Notes Mech Eng 2023:274–84. https://doi.org/10.1007/978-3-031- 40920-2_29.

[20] Huang D, Suarez D, Kang P, Ehmann K, Cao J. Robot forming: automated english wheel as an avenue for flexibility and repeatability. Manuf Lett 2023;35:342–9. https://doi.org/10.1016/j.mfglet.2023.08.104.

[21] Zhang Y, Suarez D, Ehmann K, Cao J, Guo P. In-process part tracking and shape measurement using vision-based motion capture for automated english wheeling. NAMRC 2024 (accepted).

[22] Hou Y, Min J, Lin J, Liu Z, Carsley JE, Stoughton TB. Springback prediction of sheet metals using improved material models. Procedia Eng 2017;207:173–8. https://doi.org/10.1016/j.proeng.2017.10.757.

[23] Yoshida F, Barlat F, Moon YH, Lee MG. Material models for accurate simulation of sheet metal forming and Springback. AIP Conf Proc 2010. https://doi.org/ 10.1063/1.3457626.

[24] Zhang Q, Meng W, Luo Y. Hardening behavior and model of a 316L sheet considering Macro and micro size effects. Metals 2023;13:1926. https://doi.org/10.3390/met13121926.

[25] Benton Jr K, Dewberry N, Jiaswal C, Chowdhury S, Alhmoud I, Suarez D, Ehmann K, Cao J, Gokaraju B. Initial framework design of a digital twin mixed- reality-application on human-robot bi-directional collaboration for forming double curvature plate. NAMRC 2024 (accepted).

[26] Sun Z, Zhang R, Zhu X. The progress and trend of digital twin research over the last 20 years: a Bibliometrics-based visualization analysis. J Manuf Syst 2024;74:1–15. https://doi.org/10.1016/j.jmsy.2024.02.016.

[27] de Giorgio A, Monetti FM, Maffei A, Romero M, Wang L. Adopting extended [29] Hong Y, He X, Xu J, Yuan R, Lin K, Chang B, et al. AF-FTTSnet: an end-to-end two- reality? A systematic review of manufacturing training and teaching applications. stream convolutional neural network for online quality monitoring of robotic J Manuf Syst 2023;71:645–63. https://doi.org/10.1016/j.jmsy.2023.10.016. welding. J Manuf Syst 2024;74:422–34. https://doi.org/10.1016/j.

[28] Cimino A, Longo F, Mirabelli G, Solina V, Verteramo S. An ontology-based, jmsy.2024.04.006.
general-purpose and industry 4.0-ready architecture for supporting the smart [30] Chevret S, Tiba I, Ayed Y, Maldonado D, Le VD, Balan T, et al. Robotic SPIF operator (part II – virtual reality case). J Manuf Syst 2024;73:52–64. https://doi. numerical chain development and validation. Lect Notes Mech Eng 2023:791–8. org/10.1016/j.jmsy.2024.01.001. https://doi.org/10.1007/978-3-031-41023-9_80.